



東北大學
TOHOKU UNIVERSITY

SPACE ROBOTICS LAB - SATELITE TEAM
TOHOKU UNIVERSITY - COLABS PROGRAM
FINAL REPORT

Computer Modeling and Simulation of ALEe
Micro Satellite's Orbit Decay

Student

Elion Mehdi

Supervisor

Yoshida Kazuya



August 9th 2018

Abstract

So far, artificial satellites have been used for a large range of applications, from telecommunications, to study of space environments, astronomy and meteorology. Nonetheless, the Japanese company named "ALE" (which stands for "Astro Live Experiences") imagined a new purpose for satellites : entertainment through the creation of artificial shooting stars, which consist in tiny pellets shot from satellites and burning while entering the atmosphere. ALE, along with laboratories from Tohoku University, Tokyo Metropolitan University, Kanagawa Institute of Technology and Nihon University, is working to release the first artificial shooting stars in 2019 above Hiroshima.

Within the frame of this project, an attempt is made to develop a standalone separable de-orbiting module (SDOM) in order to enable micro satellites to lower their orbit altitude down to the one from which they can shoot projectiles. This SDOM, which is a first of its kind, will be tried on ALEe micro satellite by early 2019. If successful, this will considerably reduce launching costs by enabling the company to "annex" its satellite to launching vehicles that are mostly paid by bigger customers to reach higher altitudes.

To develop such a module, concurrently with the mechanical and electronic designs of the satellite and SDOM, some numerical simulations need to be run beforehand, not only to prove this module efficient for orbit decay, but also to estimate the necessary time span to complete the desired orbit decay, and to decide on some dimensions and parameters of the system.

My assignment basically consists in developing and implementing a numerical model of ALEe micro satellite and its SDOM to simulate the orbit decay over time. Since some parts of the satellite's design and orbit plan are still likely to be modified, we will focus mostly on algorithmics, modeling and computation rather than trying to determine the actual behavior and path of the satellite, which will be done once the designs are definitively decided.

This report aims at presenting the research I have contributed to and the work I've done so far. Firstly, I will provide an overview of this project. Then, I will introduce the physical model use to run simulations and the results that came out of it. Finally, I will put forward some conclusions as for the mission itself.

Notations

Let $n \in \mathbb{N}$ such that $n \geq 2$

Let $A = (a_{ij})_{(i,j) \in [|1,n|]^2}$ and $B = (b_{ij})_{(i,j) \in [|1,n|]^2}$ des matrices with coefficients in \mathbb{R}

Let E and F be two sets.

Let $\vec{u} = [u_1 \ u_2 \ u_3]$, $\vec{v} = [v_1 \ v_2 \ v_3]$ be two vectors of \mathbb{R}^3 and $(e_0, f_0) \in \mathbb{R}^2$

Let $q = [e_0, \vec{u}]$ and $p = [f_0, \vec{v}]$ be two quaternions

For readability purposes, we will use, in this report, and provided that they are mathematically defined, the following notations :

- For $\alpha \in \mathbb{R}$, $A \curlywedge \alpha = (a_{ij}^\alpha)_{(i,j) \in [|1,n|]^2}$
- $A \otimes B = (a_{ij} \times b_{ij})_{(i,j) \in [|1,n|]^2}$
- ${}^t A = (a_{ji})_{(i,j) \in [|1,n|]^2}$
- For $p \in \mathbb{N}^*$, $\|A\|_p = \left(\sum_{(i,j) \in [|1,n|]^2} |a_{ij}|^p \right)^{\frac{1}{p}}$
- $\mathcal{F}(E, F)$ is the set of functions from set E to set F
- $\vec{u} \cdot \vec{v}$ is the dot product of \vec{u} and \vec{v}
- $\vec{u} \wedge \vec{v}$ is the cross product of \vec{u} and \vec{v}
- $\|q\| = \sqrt{e_0^2 + \vec{u} \cdot \vec{u}}$ is the norm of quaternion q
- $q \triangle p = [e_0 f_0 - \vec{u} \cdot \vec{v}, e_0 \vec{v} + f_0 \vec{u} + \vec{u} \wedge \vec{v}]$ is the Grassmann product of q and p

Table of Contents

1	Introduction	4
1.1	Context	4
1.2	Mission.....	5
1.3	Research and Objectives	8
2	Preliminary study of the N-body Problem.....	9
2.1	Physical Model.....	9
2.2	Mathematical Model	10
2.3	Numerical Model.....	11
3	Rigid Model of the Satellite	13
3.1	Description of the System	13
3.2	Frame of Study	15
3.3	Forces Acting on an Earth-orbiting Satellite.....	17
3.3.1	Gravity	17
3.3.2	Atmospheric Drag	19
3.3.3	Solar Radiation Pressure	22
3.3.4	Magnetic Field.....	24
3.4	Equations of motion	25
4	Improved Model of the Satellite	26
4.1	Mass-Spring Network Approximation	26
4.2	Internal Forces	29
4.3	Modified Computation of SRP and Drag Forces	31
4.4	Equations of Film Behavior.....	32
5	Results and Discussions	33
5.1	Results	33
5.2	Potential Improvements.....	36
6	Conclusion	36
	References	37

1 Introduction

This section lays an overview of the project's whys and wherefores. First of all, the context is briefly summarized. Secondly, the mission itself is described and, finally, the very research I have been involved in and its objectives are detailed.

1.1 Context

The ALE Company and its goal

ALE is a Japan-based space entertainment startup that creates shooting stars on demand using microsatellites to shoot particles that will burn in the upper part of the atmosphere. It was founded in September 2011 by Lena Okajima, an entrepreneur with a Ph.D. in Astronomy from the University of Tokyo. Its mission is to contribute to scientific research through entertainment. Indeed, besides entertainment purposes, ALE also aims at better understanding of naturally occurring shooting stars and meteorites, studying the upper atmosphere where the projectiles will burn, which is still one of the least understood parts of the atmosphere, as well as further comprehending orbital mechanics of space debris.



ALE's Organization Chart



Dr. Lena Okajima
CEO
Founder



Dr. Toshinori Kuwahara
CTO
Tohoku University, Department
of Aerospace Engineering



Dr. Hironori Sahara
Tokyo Metropolitan University
Division of Aerospace
Engineering



Dr. Takeo Watanabe
Kanagawa Institute of Technology
Department of Mechanical
Engineering



Dr. Shinsuke Abe
Nihon University
Department of Aerospace
Engineering

ALE's protagonists and partners

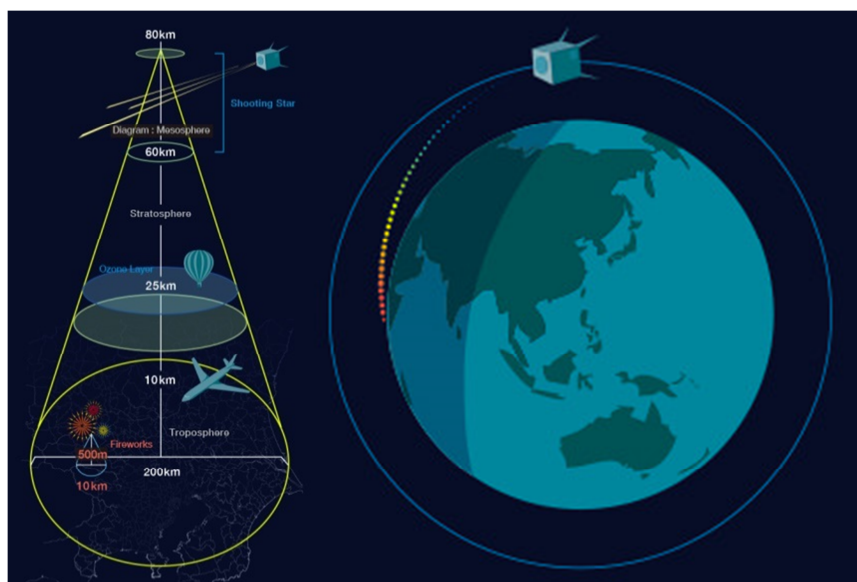
To achieve its goal, ALE benefits from the help of both economic and research partners. Family Mart and Japan Airlines rank among the biggest economic partners of ALE. As for the scientific partners, laboratories from several Japanese Universities are involved, each one being assigned with a particular research task:

- Tohoku University : Mechanical and Electronical Design and Manufacturing, Communications, Orbit Calculation
- Tokyo Metropolitan University : Orbital Simulation、Thermal Analysis
- Kanagawa Institute of Technology ; Material Analysis、Structural Analysis
- Nihon University : Luminescence Observation、Material Development

1.2 Mission

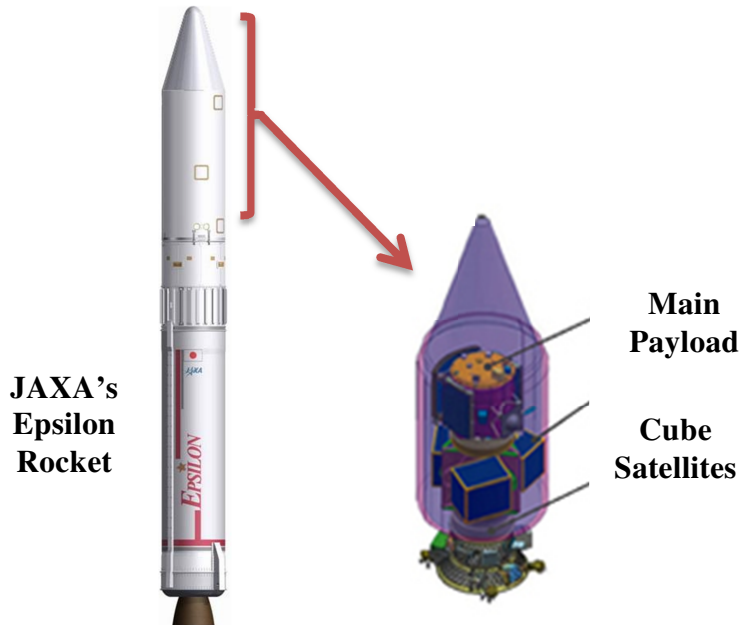
Create Shooting stars

Natural shooting stars occur when particles of several millimeters in size enter the Earth's atmosphere and burn while emitting bright light called plasma emission. To reproduce that phenomenon artificially, ALE will use an orbiting micro satellite loaded with tiny projectiles which will be shot into the upper atmosphere and burn, thus reproducing the appearance of a shooting star.



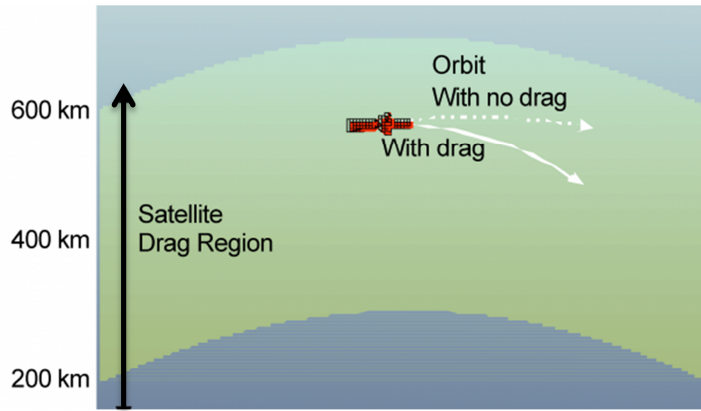
Micro Satellites

To create such artificial shooting stars on command, several micro satellites will be used, which include ALEX, launched by SpaceX, and ALEe, launched by JAXA's Epsilon rocket. Unlike ALEX, ALEe will be deployed at an altitude of 500 km, which is 100 km higher than its final orbiting altitude because it has been "annexed" to another launch contract to reduce launch costs.



De-Orbiting Module

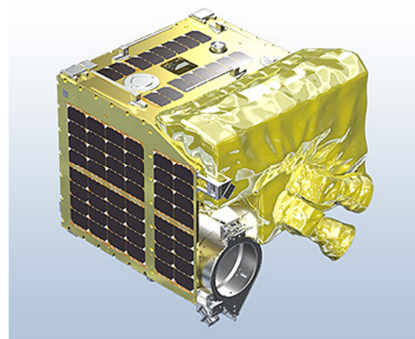
Before shooting projectiles, the micro satellite has to settle into a stable orbit around Earth, at approximately 400 km of altitude. The first solution is to use a launching vehicle that will directly deploy the satellite at its cruising altitude of 400 km. This solution, although quite expensive, has already been adopted out of security. Meanwhile, an attempt is made to develop a standalone separable de-orbiting module (SDOM) to decrease the satellite's altitude from 500 km (deployment altitude) to approximately 400 km (cruising altitude) using atmospheric drag (which slows the satellite and, therefore, causes altitude loss). If successful, this procedure will allow ALE's micro satellite to annex itself to any launching vehicle mostly paid by bigger customers to be deployed at a higher altitude, which would considerably reduce the launching costs.



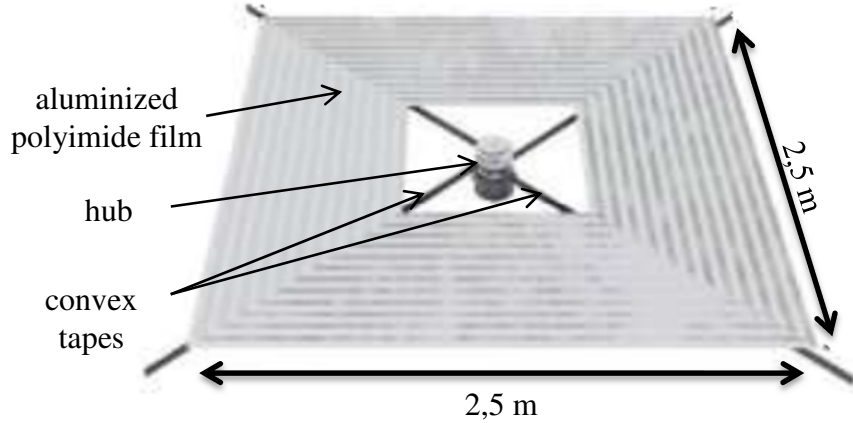
A similar attempt has been made with FREEDOM CubeSat made by Nakashimada Engineering Works and Tohoku University. This CubeSat re-entered the atmosphere on February 5, 2017 after only three weeks in orbit, indicating its drag sail was successful in rapidly removing the small satellite from orbit [1]. Here's a picture of FREEDOM's de-orbiting module.



However, this satellite used a de-orbiting module (DOM) that was not separable since it was not intended to re-orbit after losing altitude. In the case of ALEe, the satellite must re-orbit after losing altitude. To do so, the deployed module must be detached from the CubeSat, hence the name of this SDOM module.



The SDOM is beforehand contained in a cylinder shaped mechanism. After deployment, the SDOM consists in a thin aluminized polyimide film supported by four diagonal deployable masts and linked to the micro satellite by three convex tapes.



1.3 Research and Objectives

Once deployed, the SDOM is expected to slow down the satellite by using the drag force exerted on the film by Earth's atmosphere. However, the behavior of the whole system {Satellite + Deployed SDOM} is quite hard to predict, mostly owing to the non-rigidity of the convex tapes and film. Thus, in order to decide of some parameters and dimensions of the SDOM, such as boom length (length of the convex tapes linking the film to the satellite), numerical simulations need to be run. Those simulations will allow us to estimate the trajectory and attitude of the system during the orbit decay, as well as the time span thereof, which is critical to meet the deadlines for the first artificial meteor showers.

Firstly, we will introduce a model for N-body problems that will be useful to determine the positions of planets and the trajectory of the satellite.

Secondly, we will introduce a rigid-body model of the system based on Euler equations, after which we will propose an improvement of that model taking into account the flexibility of the film.

Finally, we will draw conclusions from that study as for its results and potential further improvements.

2 Preliminary study of the N-body Problem

In this section, we introduce a model to numerically solve N-body problems. This model will thereafter be useful for determining the positions of the solar system's planets and the satellite.

2.1 Physical Model

Generally speaking, an N-body problem consists in a set of N bodies distributed in space and interacting with each other according to a given law. In this case, we will deal with an N-body problem, described as "gravitational" because it is ruled by Newton's law of universal gravitation, within the frame of non-relativistic mechanics.

Let's consider a set of N point bodies, indexed with $i \in [|1, N|]$ and of masses $m_i, i \in [|1, N|]$. These bodies interact with each other according to Newton's law of universal gravitation. The application of Newton's law of motion on each of the N bodies in an inertial frame $\mathcal{R}(O, \vec{e}_x, \vec{e}_y, \vec{e}_z)$ allows us to get the following differential equations system :

$$\forall i \in [|1, N|], \quad \vec{a}_i = \sum_{j \in [|1, N|] \setminus \{i\}} \overrightarrow{q_{j \rightarrow i}}$$

with

- $\overrightarrow{q_{j \rightarrow i}}$ the gravitational field exerted by body j on body i
- $\vec{a}_i = {}^t[\ddot{x}_i \quad \ddot{y}_i \quad \ddot{z}_i]$ the acceleration of body i

The law of gravitation gives us the expression for this gravitational field :

$$\forall (i, j) \in [|1, N|]^2, \quad \overrightarrow{q_{j \rightarrow i}} = \frac{-Gm_j}{d_{ij}^3} \overrightarrow{P_j P_i}$$

with

- $d_{ij} = \sqrt{(x_j - x_i)^2 + (y_j - y_i)^2 + (z_j - z_i)^2}$ the distance between bodies i and j
- $P_i = {}^t[x_i \quad y_i \quad z_i]$ the position vector of body i
- $G = 6.67408 \times 10^{-11} \text{ m}^3 \cdot \text{kg}^{-1} \cdot \text{s}^{-2}$ the gravitational constant

We finally get a system of N vectorial differential equations of unknowns are P_i and \dot{P}_i , $i \in [|1, N|]$.

2.2 Mathematical Model

Given that we will use Matlab and C++ in this project, a matrix formalism requiring a minimum of iterative loops will be more appropriate.

The Cauchy problem obtained at the end of physical model is the following :

$$(C_0) \quad \begin{cases} \dot{U}(t) = f(t, U(t)) & t \in [0, T] \\ U(0) = U_0 \in \mathbb{R}^{6N} \end{cases}$$

with • $U \in \mathcal{F}([0, T], \mathbb{R}^{6N})$ such that $\forall t \in [0, T]$, $U(t) = \begin{bmatrix} X(t) \\ Y(t) \\ Z(t) \\ \dot{X}(t) \\ \dot{Y}(t) \\ \dot{Z}(t) \end{bmatrix}$

- $X = {}^t[x_1 \dots x_N]$, $Y = {}^t[y_1 \dots y_N]$, $Z = {}^t[z_1 \dots z_N]$, $M = {}^t[m_1 \dots m_N]$

- $f \in \mathcal{F}([0, T] \times \mathbb{R}^{6N}, \mathbb{R}^{6N})$ such that $\forall t \in [0, T]$, $f(t, U(t)) = \begin{bmatrix} \dot{X}(t) \\ \dot{Y}(t) \\ \dot{Z}(t) \\ \ddot{X}(t) \\ \ddot{Y}(t) \\ \ddot{Z}(t) \end{bmatrix}$

An important step in this method consists in matrix calculating vectors \ddot{X} , \ddot{Y} et \ddot{Z} knowing Newton's law of motion provides an expression of those (and therefore of f) :

$$\forall i \in [|1, N|], \quad \begin{cases} \ddot{x}_i = \sum_{j \in [|1, N|] \setminus \{i\}} q_{x j \rightarrow i} & \text{où } q_{x i \rightarrow j} = \frac{-Gm_j}{d_{ij}^3} (x_i - x_j) \\ \ddot{y}_i = \sum_{j \in [|1, N|] \setminus \{i\}} q_{y j \rightarrow i} & \text{où } q_{y i \rightarrow j} = \frac{-Gm_j}{d_{ij}^3} (y_i - y_j) \\ \ddot{z}_i = \sum_{j \in [|1, N|] \setminus \{i\}} q_{z j \rightarrow i} & \text{où } q_{z i \rightarrow j} = \frac{-Gm_j}{d_{ij}^3} (z_i - z_j) \end{cases}$$

The expression of f doesn't depend on t , so we will indifferently write $f(t, U(t)) = f(U(t))$.

2.3 Numerical Model

Implementation of motion equations

First of all, let's note that :

$$\begin{aligned}\ddot{X} &= Q_x E \\ \ddot{Y} &= Q_y E \\ \ddot{Z} &= Q_z E\end{aligned}$$

where $\bullet \cdot E = {}^t[1 \ 1 \ \dots \ 1] \in \mathbb{R}^N$

- $\forall a \in \{x, y, z\}$, $Q_a \in \mathcal{M}_N(\mathbb{R})$ defined by $[Q_a]_{ij} = \begin{cases} q_{a \ j \rightarrow i} & \text{si } i \neq j \\ 0 & \text{si } i = j \end{cases}$

Thus, the method consists in matrix calculating the Q_a , $a \in \{x, y, z\}$ with the available data which is M , X , Y and Z .

To do so, we define the following matrices (which we can build by repeating X , Y , Z and M columns) :

$$C_M = \begin{pmatrix} m_1 & \cdots & m_1 \\ \vdots & \ddots & \vdots \\ m_N & \cdots & m_N \end{pmatrix}$$

$$C_a = \begin{pmatrix} a_1 & \cdots & a_1 \\ \vdots & \ddots & \vdots \\ a_N & \cdots & a_N \end{pmatrix}, \quad a \in \{x, y, z\}$$

Then we define the matrices :

$$D_a = C_a - {}^t C_a = (a_i - a_j)_{(i,j) \in [|1,N|]^2}, \quad a \in \{x, y, z\}$$

Afterwards, we can define the distance matrix :

$$D = (d_{ij})_{(i,j) \in [|1,N|]^2} = (D_x \otimes D_x + D_y \otimes D_y + D_z \otimes D_z) \wedge \left(\frac{1}{2}\right)$$

We can finally matrices Q_a , $a \in \{x, y, z\}$ making sure to replace diagonal elements of matrix $D \wedge (-3)$ not to end up with infinity values.

$$\forall a \in \{x, y, z\}, \quad Q_a = -G \times (D \wedge (-3)) \otimes {}^t C_M \otimes D_a$$

Note that the method to calculate \ddot{X} , \ddot{Y} and \ddot{Z} is the same, which makes this algorithm potentially parallelizable.

Choice of ODE solver

Let $h \in [0, T]$ a time step and $(t_n)_{n \in [|0, \frac{T}{h}|]}$ a discretization of $[0, T]$ defined by $\forall n \in [|0, \frac{T}{h}|], t_n = nh$. For $n \in \mathbb{N}$, let $U^n \in \mathbb{R}^{6N}$ be the approximation of $U(t_n)$ where U is the exact solution to the Cauchy problem (C_0) . Within the frame of this project, we will use Runge-Kutta 4 to solve the ODEs.

$$\text{Runge-Kutta 4 (RK4)} : \left\{ \begin{array}{l} k_1 = f(t_n, U^n) \\ k_2 = f(t_n + \frac{h}{2}, U^n + \frac{h}{2}k_1) \\ k_3 = f(t_n + \frac{h}{2}, U^n + \frac{h}{2}k_2) \\ k_4 = f(t_n + h, U^n + hk_3) \\ U^{n+1} = U^n + \frac{h}{6}(k_1 + 2k_2 + 2k_3 + k_4) \\ U^0 = U_0 \end{array} \right.$$

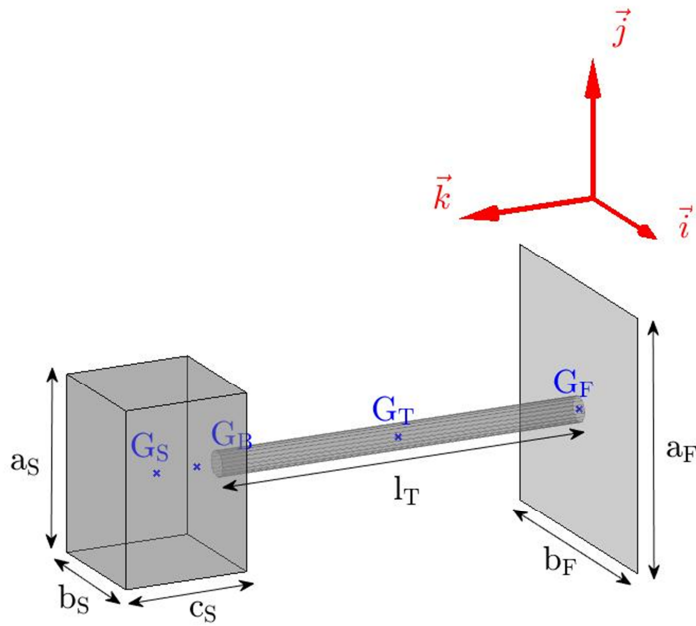
Let's remind ourselves that the total accumulated error with this method is of order $O(h^4)$.

3 Rigid Model of the Satellite

In this section, we will focus specifically on building a model for the trajectory and attitude of the {Satellite + deployed DOM} system. Such a model is not straightforward to conceive, particularly because of the flexibility of the film and tapes. Therefore, we will start by building a rigid-body model based on Euler equations that we will thereafter try to improve.

3.1 Description of the System

To start simple, we will consider that the {Satellite + Deployed SDOM} system is one rigid body made up of a tape, a satellite and a film. Then we associate a body-fixed frame (BRF) to this system, as illustrated in the sketch below.



Unit vectors \vec{i} , \vec{j} , \vec{k} are defined along the principal axes of the system and form an orthonormal basis for the body fixed reference frame : \vec{k} is defined along the tape axis, \vec{i} and \vec{j} are defined as orthogonal to \vec{k} along the two other satellite directions.

This frame forms an orthonormal basis for the body-fixed reference frame $\mathcal{R}_B(G_B, \vec{i}, \vec{j}, \vec{k})$ (where G_B is the barycenter of the whole system) and allows us to define the dimensions of the system :

Satellite

- a_S : dimension along the \vec{j} direction (fixed to 0.7 m for all the following simulations)
- b_S : dimension along the \vec{i} direction (fixed to 0.5 m for all the following simulations)
- c_S : dimension along the \vec{k} direction (fixed to 0.5 m for all the following simulations)

Film

- a_F : dimension along the \vec{j} direction (fixed to 2.5 m for all the following simulations)
- b_F : dimension along the \vec{i} direction (fixed to 2.5 m for all the following simulations)

Tape

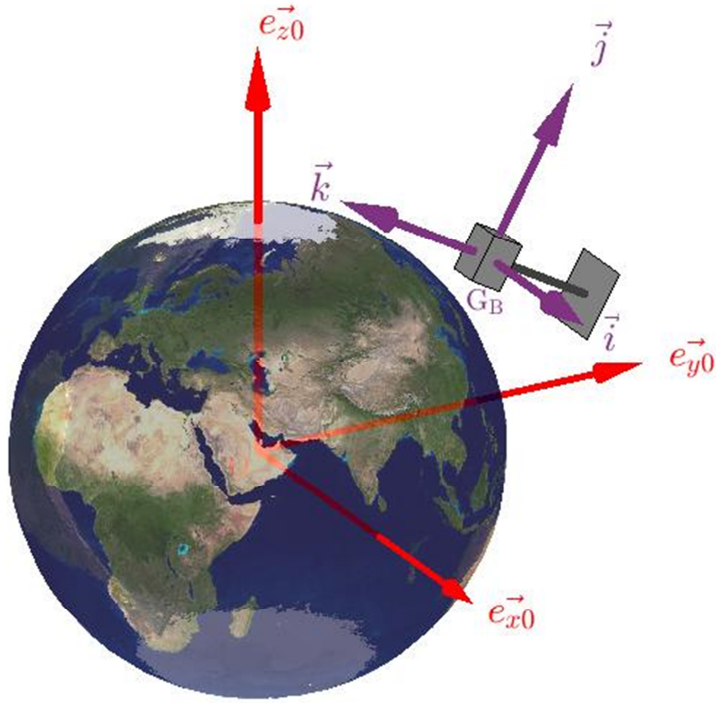
- l_T : dimension along the \vec{k} direction (variable between 2.0 m and 5.0 m)

Along the dimensions of the satellite, we will also need the mass properties of the system (note that their values are given by both experiments and SolidWorks 3D models) :

- (G_S, m_S) : mass and barycenter of the satellite
- (G_T, m_T) : mass and barycenter of the tape
- (G_F, m_F) : mass and barycenter of the film
- $m_B = m_S + m_T + m_F$: total mass (fixed to 65.06 kg for all the following simulation)
- $G_B = \frac{1}{m_B}(m_S G_S + m_T G_T + m_F G_F)$: barycenter of the whole system
- $I_{G_B} = I(G_B)_{(\vec{i}, \vec{j}, \vec{k})}$: inertia matrix about G_B expressed in the BRF (depends on l_T)

3.2 Frame of Study

This study consists in determining the motion of the system in a three-dimensional space. We will study the movement of the system the Earth-Centered Inertial (ECI) frame of reference $\mathcal{R}_0(O, \vec{e}_{x0}, \vec{e}_{y0}, \vec{e}_{z0})$ defined as illustrated below.



O is the Earth's center of mass. \vec{e}_{x0} and \vec{e}_{y0} are contained in the equatorial plane. \vec{e}_{z0} is aligned with the Earth's spin axis or celestial North Pole.

The system has a total of 6 degrees of freedom : 3 of translation and 3 of rotation (also called attitude).

Translation

To describe the translation of the system, we will consider the position of its center of mass G_B in reference to the ECI frame. Let $\vec{R}_B = [x_B, y_B, z_B]$ and $\vec{V}_B = [v_x, v_y, v_z]$ be G_B 's position and velocity vectors in the ECI coordinate system. These will be the unknown variables as for the translation part of the system's motion.

Attitude

To describe the attitude of the system, we will consider rotation of the BRF basis $(\vec{i}, \vec{j}, \vec{k})$ in reference to the ECI basis $(\vec{e}_{x0}, \vec{e}_{y0}, \vec{e}_{z0})$. To do so, we will use a quaternion-based representation of the system's attitude because they are known for being numerically more stable than Euler angles for example.

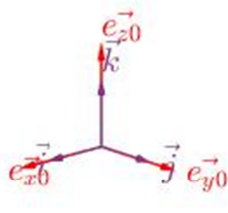
Let $q = [e_0 \ e_1 \ e_2 \ e_3]$ be the unit quaternion, which means $\|q\| = 1$, representing the rotation of $(\vec{i}, \vec{j}, \vec{k})$ in reference to $(\vec{e}_{x0}, \vec{e}_{y0}, \vec{e}_{z0})$. Since q is a unit quaternion, it can also be written $q = [\cos(\frac{\alpha}{2}), \sin(\frac{\alpha}{2}) \vec{u}]$ where α is the rotation angle of $(\vec{i}, \vec{j}, \vec{k})$ around unit vector \vec{u} , assuming that BFR and ECI bases initially coincide.

To the unit quaternion q we can associate the rotation matrix :

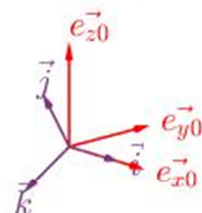
$$R_q = \begin{pmatrix} e_0^2 + e_1^2 - e_2^2 - e_3^2 & 2(e_1 e_2 - e_0 e_3) & 2(e_0 e_2 + e_1 e_3) \\ 2(e_0 e_3 + e_1 e_2) & e_0^2 - e_1^2 + e_2^2 - e_3^2 & 2(e_2 e_3 - e_0 e_1) \\ 2(e_1 e_3 - e_0 e_2) & 2(e_0 e_1 + e_2 e_3) & e_0^2 - e_1^2 - e_2^2 + e_3^2 \end{pmatrix}$$

Here are some examples of quaternion based rotations :

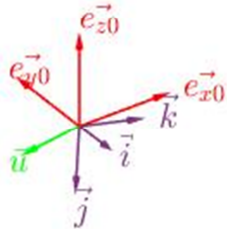
Initial state



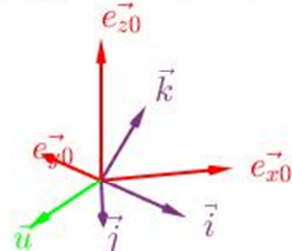
$\vec{u} = \vec{e}_{x0}, \alpha = 2\pi/3$



$\vec{u} = \sqrt{1/3}(\vec{e}_{x0} + \vec{e}_{y0} + \vec{e}_{z0}), \alpha = 3\pi/4$



$\vec{u} = \sqrt{1/3}(\vec{e}_{y0} - \vec{e}_{x0} - \vec{e}_{z0}), \alpha = \pi/3$



We will also need the system's angular velocity vector $\vec{\omega}_B = [\omega_1 \ \omega_2 \ \omega_3]$ which represents the rotation velocity of BRF in reference to ECI.

3.3 Forces Acting on an Earth-orbiting Satellite

In this section, we will provide a general description of the different forces the system is subject to. We will also estimate some orders of magnitude to get an idea of their relative importance in the case of our system.

3.3.1 Gravity

Principle

For each attractor i of mass M_i whose center of mass is located at P_i , the system is subject to a force $\overrightarrow{F_{grav,i}}$ given by :

$$\overrightarrow{F_{grav,i}} = \frac{-GM_i m_B}{\|P_i G_B\|^3} \overrightarrow{P_i G_B}$$

This force also causes a gravity gradient torque whose expression, in the BRF coordinates system, is given by :

$$\overrightarrow{M_{grav,i}} = \frac{3GM_i}{\|P_i G_B\|^5} \begin{pmatrix} YZ(I_3 - I_2) \\ XZ(I_1 - I_3) \\ XY(I_2 - I_1) \end{pmatrix}_{(\vec{i}, \vec{j}, \vec{k})}$$

where • $I_{G_B} = I(G_B)_{(\vec{i}, \vec{j}, \vec{k})} = \begin{pmatrix} I_1 & 0 & 0 \\ 0 & I_2 & 0 \\ 0 & 0 & I_3 \end{pmatrix}$ • $\overrightarrow{P_i G_B} = [X \ Y \ Z]_{(\vec{i}, \vec{j}, \vec{k})}$

Order of Magnitude

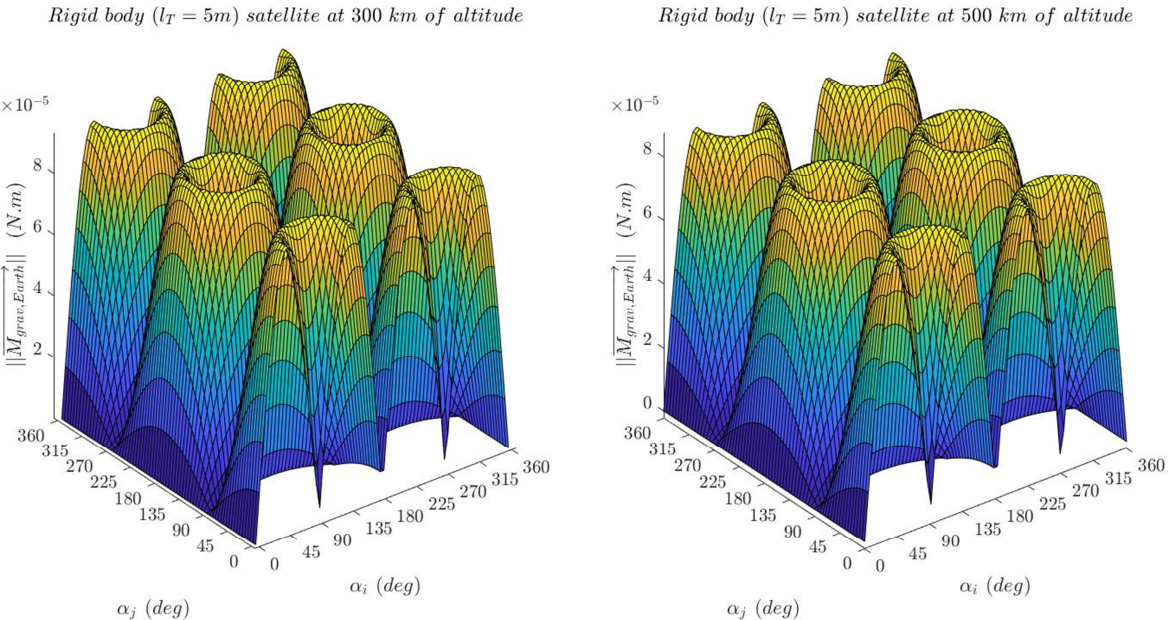
Within the frame of this project, we will consider Earth, Sun and Moon as gravitational attractors acting on the system. For an Earth-orbiting system, assuming its altitude ranges from 300 km to 500 km, the gravitation forces and torques applied on it will have the following orders of magnitude :

$$\|\overrightarrow{F_{grav,Earth}}\| \approx 5.8 \times 10^2 \text{ N} , \quad \|\overrightarrow{F_{grav,Moon}}\| \approx 2.2 \times 10^{-2} \text{ N} , \quad \|\overrightarrow{F_{grav,Sun}}\| \approx 3.9 \times 10^{-1} \text{ N}$$

As for the gravity gradient torque, its value strongly depends on the system's altitude and attitude. Let's make a few assumptions to calculate an order of magnitude of the drag force and torque :

- $l_T = 5 \text{ m}$
- the system's BRF initially coincides with the orbit reference frame (\vec{k} directed like $\overrightarrow{V_B}$)

Since the system is quite symmetrical around \vec{k} , rotation around that axis won't influence the gravity gradient torque much. We will make the satellite rotate by α_i around \vec{i} and then by α_j around \vec{j} . Here are the $\|\overrightarrow{M_{grav,Earth}}\|$ graphs we obtain for initial altitudes of 500 km and 300 km :



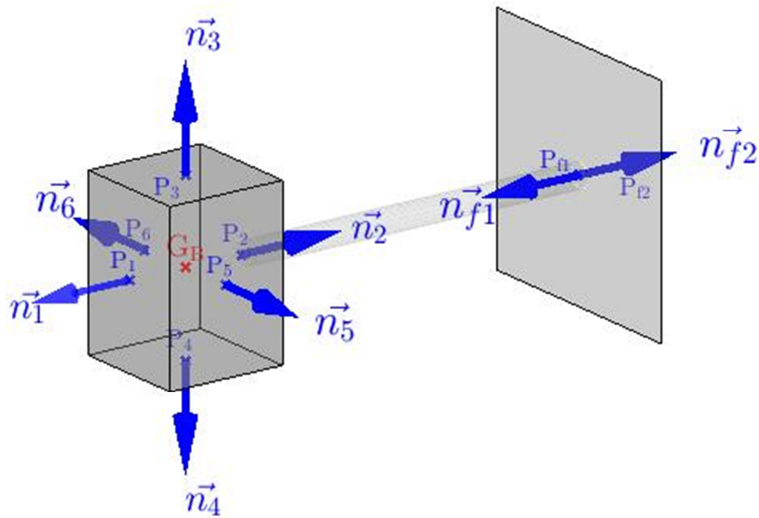
These graphs suggest that the gravity gradient torque has stable equilibrium points that correspond to its minimum values, as well as unstable equilibrium points for its maximum values. The orders of magnitude found for this system are given in the table below :

	altitude of 300 km		altitude of 500 km	
	min	max	min	max
$\ \overrightarrow{M_{grav,Earth}}\ \text{ (N.m)}$	3.4×10^{-9}	9.3×10^{-5}	3.1×10^{-9}	8.5×10^{-5}
$\ \overrightarrow{M_{grav,Moon}}\ \text{ (N.m)}$	8.9×10^{-15}	6.1×10^{-12}	6.0×10^{-15}	6.0×10^{-12}
$\ \overrightarrow{M_{grav,Sun}}\ \text{ (N.m)}$	1.1×10^{-16}	2.9×10^{-12}	1.1×10^{-16}	2.7×10^{-12}

3.3.2 Atmospheric Drag

Principle

This force results from the interaction between the system's faces and the upper atmosphere. For this system, we consider 8 faces indexed with $i \in [|1,6|] \cup [f_1, f_2]$. For each one of these faces, we define an orthogonal unit vector \vec{n}_i and a center of pressure P_i located at the center of the face, as illustrated below.



- Let
- \vec{V}_{P_i} be the velocity of the center of pressure i with reference the atmosphere
 - $\vec{V}_{atm,i}$ be the velocity of the atmosphere with reference to face i
 - \vec{V}_B be the velocity of the system's center of mass G_B with reference to the Earth
 - $\vec{\omega}_B$ be the angular velocity vector of BRF with reference to ECI

In practice, we will make the following assumptions :

- the velocity of the atmosphere with reference to Earth is negligible compared to \vec{V}_B
- $\forall i \in [|1,6|] \cup \{f_1, f_2\}$, $\|\vec{G}_B \vec{P}_i \wedge \vec{\omega}_B\| \ll \|\vec{V}_B\|$

The first assumption allows us to write :

$$\vec{V}_{atm,i} = -\vec{V}_{P_i} = -(\vec{V}_B + \vec{G}_B \vec{P}_i \wedge \vec{\omega}_B)$$

The second assumption justifies the approximation of the total drag force applied on face i (rigorously obtained by integrating infinitesimal forces over the face) by one single force applied on P_i whose expression is given by :

$$\overrightarrow{F_{drag,i}} = \begin{cases} -\frac{1}{2} c_{D_i} \rho A_i \|\overrightarrow{V_{atm,i}}\|^2 \cos(\alpha_i) \overrightarrow{v_{atm,i}} & \text{if } \cos(\alpha_i) < 0 \\ \vec{0} & \text{otherwise} \end{cases}$$

where :

- A_i is the area of face i
- $\overrightarrow{v_{atm,i}} = \frac{\overrightarrow{V_{atm,i}}}{\|V_{atm,i}\|}$
- $\alpha_i = (\overrightarrow{V_{wind,i}}, \overrightarrow{n_i})$ is the angle between $\overrightarrow{V_{P_i}}$ and $\overrightarrow{n_i}$
- c_{D_i} is the drag coefficient of face i (≈ 2 for each face)
- ρ is the air density calculated with 1976 Standard Atmosphere model (depends on the position of the satellite)

The condition $\cos(\alpha_i) < 0$ ensures that face i is actually facing the wind, without which face i is shaded by another face, which entails $\overrightarrow{F_{drag,i}} = \vec{0}$.

Thereafter, we can calculate the moment associated to $\overrightarrow{F_{drag,i}}$ by G_B :

$$\overrightarrow{M_{drag,i}} = \overrightarrow{G_B P_i} \wedge \overrightarrow{F_{drag,i}}$$

Finally, we can calculate the total drag force and torque applied on the system follows :

$$\overrightarrow{F_{drag}} = \sum_{i \in [|1,6|] \cup \{f_1, f_2\}} \overrightarrow{F_{drag,i}}$$

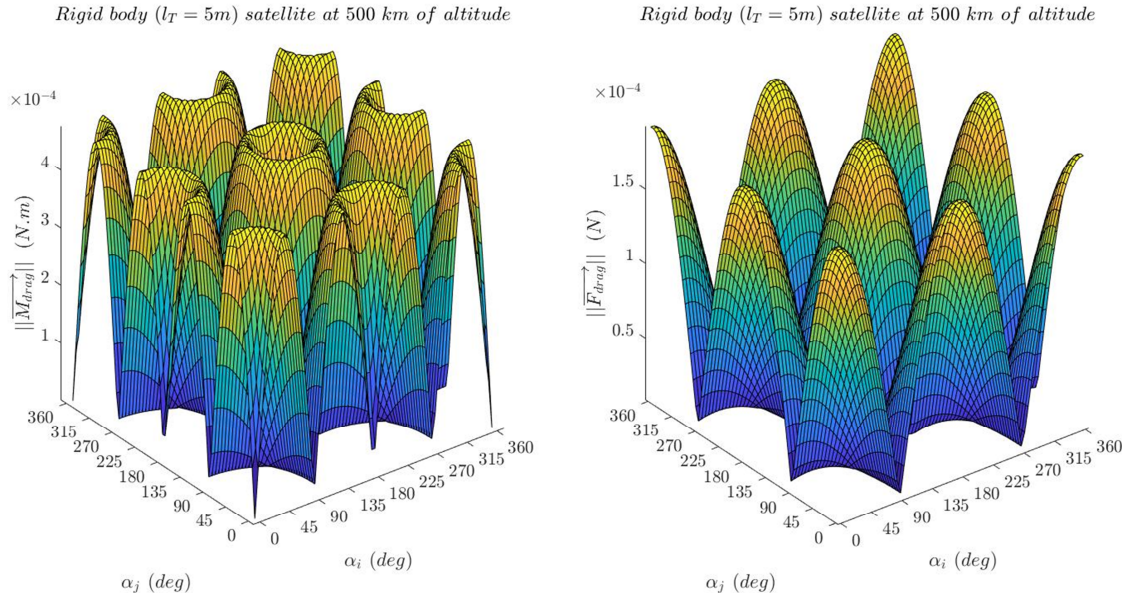
$$\overrightarrow{M_{drag}} = \sum_{i \in [|1,6|] \cup \{f_1, f_2\}} \overrightarrow{M_{drag,i}}$$

Order of Magnitude

For this system, the norm of $\overrightarrow{F_{drag}}$ and $\overrightarrow{M_{drag}}$ depend mostly on its altitude, attitude and velocity. Let's make a few assumptions to calculate an order of magnitude of the drag force and torque :

- the system has a circular orbit velocity around Earth and no angular velocity
- $l_T = 5 \text{ m}$
- the system's BRF initially coincides with the orbit reference frame (\vec{k} directed like $\overrightarrow{V_B}$)

Since rotation around \vec{k} doesn't influence the drag force, just as we did for the gravity gradient torque, we will make the satellite rotate around \vec{i} and then around \vec{j} . Here are the graphs we obtain for an initial altitude of 500 km :



In the same way as the gravity gradient torque, these graphs suggest that drag torque has stable and unstable equilibrium points that correspond respectively to its minimum and maximum values. However, these points are not necessarily the same for both torques. The orders of magnitude found for this system are given in the table below :

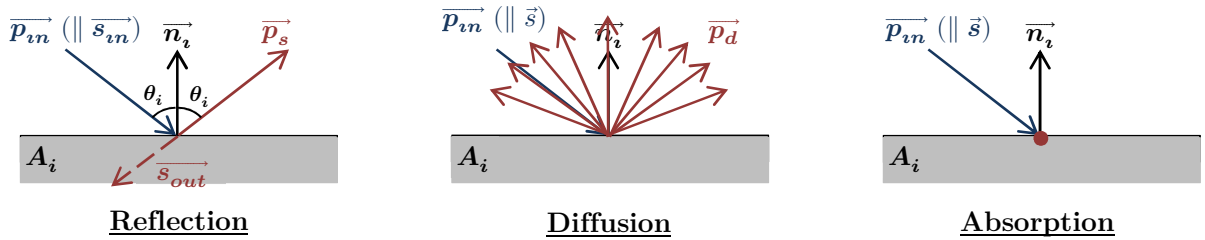
	altitude of 300 km		altitude of 500 km	
	min	max	min	max
$\ \overrightarrow{F_{drag}}\ \text{ (N)}$	2.9×10^{-4}	7.3×10^{-3}	7.9×10^{-6}	1.9×10^{-4}
$\ \overrightarrow{M_{drag}}\ \text{ (N.m)}$	1.8×10^{-9}	1.8×10^{-2}	4.9×10^{-11}	4.8×10^{-4}

3.3.3 Solar Radiation Pressure

Principle

Solar radiation force results from the impact of photons on the different surfaces of the satellite. A fraction of them, ρ_s is specularly reflected, another fraction ρ_d is diffusely reflected, and the last fraction of them, ρ_a , is absorbed. The relation between these fractions is :

$$\rho_s + \rho_a + \rho_d = 1$$



The force created by the absorbed photons results from the momentum transfer from the photons to the satellite. Thus, this force is directed along the sun line and, for each surface i , is defined by :

$$\overrightarrow{F}_{a,i} = \begin{cases} \rho_a p_{rad} A_i (-\vec{n}_i \cdot \vec{s}) \vec{s} = \rho_a p_{rad} A_i \cos(\theta_i) \vec{s} & \text{if } \cos(\theta_i) > 0 \\ \vec{0} & \text{otherwise} \end{cases}$$

where : • $\vec{s} = \frac{\vec{P}_{Sun} G_B}{\|\vec{P}_{Sun} G_B\|}$ • $p_{rad} = 4.644 \times 10^{-6} N.m^2$ is the solar radiation pressure
 • $\theta_i = (-\vec{n}_i, \vec{s})$ • A_i and n_i are the area and unit normal vector of face i

The condition $\cos(\theta_i) > 0$ ensures that face i is actually facing the sun, without which face i is shaded by another face and undergoes no radiation force.

The fraction of photons that are specularly reflected transfer twice the momentum and the direction is normal to the surface :

$$\overrightarrow{F}_{s,i} = \rho_s p_{rad} A_i (-\vec{n}_i \cdot \vec{s}_{in}) \vec{s}_{in} + \rho_s p_{rad} A_i (-\vec{n}_i \cdot \vec{s}_{out}) \vec{s}_{out}$$

Since $-\vec{n}_i \cdot \vec{s}_{in} = -\vec{n}_i \cdot \vec{s}_{out} = \cos(\theta_i)$ and $\vec{s}_{out} + \vec{s}_{in} = -2 \cos(\theta_i) \vec{n}_i$, we finally get :

$$\overrightarrow{F_{s,i}} = \begin{cases} -2\rho_s p_{rad} A_i \cos^2(\theta_i) \vec{n}_i & \text{if } \cos(\theta_i) > 0 \\ \vec{0} & \text{otherwise} \end{cases}$$

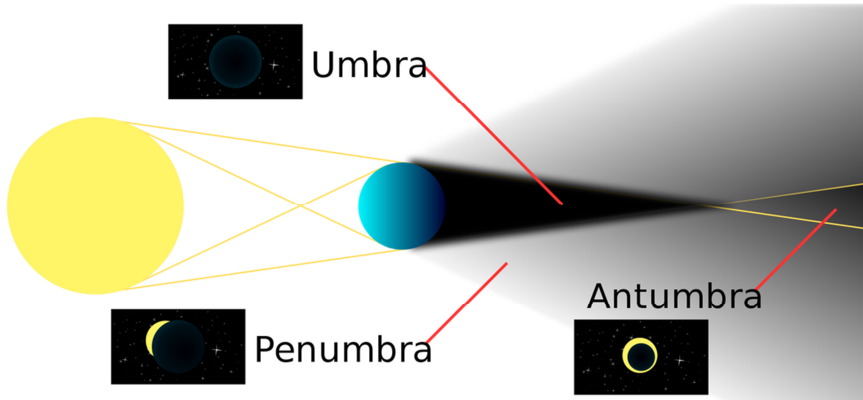
As for the force resulting from diffuse reflection, the photon's momentum may be considered as stopped at the surface, and re-radiated uniformly into the hemisphere. Thus, $\overrightarrow{F_{d,i}}$ has a component due to transfer of momentum, and another component due to re-radiation that will be normal to the surface since that re-radiation is uniform.

$$\overrightarrow{F_{d,i}} = \begin{cases} \rho_d p_{rad} A_i (-\vec{n}_i \cdot \vec{s}) (\vec{s} - \frac{2}{3}\vec{n}_i) = \rho_d p_{rad} A_i \cos(\theta_i) (\vec{s} - \frac{2}{3}\vec{n}_i) & \text{if } \cos(\theta_i) > 0 \\ \vec{0} & \text{otherwise} \end{cases}$$

The total solar radiation force on face i is given by :

$$\overrightarrow{F_{SRP,i}} = \overrightarrow{F_{a,i}} + \overrightarrow{F_{d,i}} + \overrightarrow{F_{s,i}} = \nu p_{rad} A_i \cos(\theta_i) [(1 - \rho_s) \vec{s} - (2\rho_s \cos(\theta_i) + \frac{2}{3}\rho_d) \vec{n}_i]$$

where $\nu \begin{cases} = 1 & \text{in lighted area} \\ \in [0,1] & \text{in penumbra / antumbra} \\ = 0 & \text{in umbra} \end{cases}$ is the shadow function, as illustrated below.



Just as we did for the drag force, we can calculate the moment associated to $\overrightarrow{F_{drag,i}}$ by G_B :

$$\overrightarrow{M_{SRP,i}} = \overrightarrow{G_B P_i} \wedge \overrightarrow{F_{SRP,i}}$$

Finally, we can calculate the total SRP force and torque applied on the system as follows :

$$\overrightarrow{F_{SRP}} = \sum_{i \in [1,6] \cup \{f_1, f_2\}} \overrightarrow{F_{SRP,i}}$$

$$\overrightarrow{M_{SRP}} = \sum_{i \in [1,6] \cup \{f_1, f_2\}} \overrightarrow{M_{SRP,i}}$$

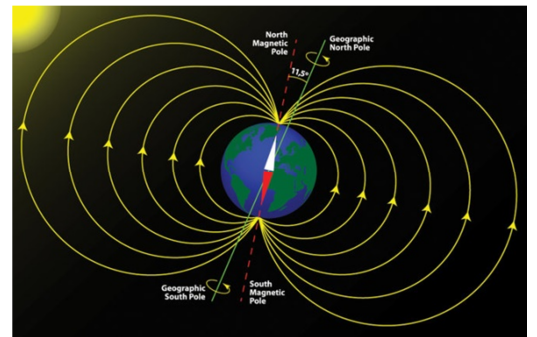
Order of magnitude

In our case, the ALEe satellite is going to operate in low Earth orbit (LEO) between altitudes of 300km and 500km. It is known that, in that area, air drag and gravity are the largest forces and torques acting on a satellite. Indeed, preliminary computations show that both SRP force and torque don't exceed the order of 10^{-5} (SI), which is below the maximum values of drag and gravity given above. Besides that, the actual orbit plan is still likely to be changed, which makes it difficult to estimate how much light the satellite is going to get. Therefore, we will neglect that force in the following simulations.

3.3.4 Magnetic Field

The Earth possesses a magnetic field that, in LEO area, can be approximated by the field of a magnetic dipole positioned at the center of the Earth and tilted at an angle of about 11.5° with respect to the rotational axis of the Earth.

That magnetic field is mostly used for attitude control through the use of magnetic torquers, according to the following formula :



$$\overrightarrow{T_{mag}} = \vec{m} \wedge \overrightarrow{B_{Earth}}$$

where • $\overrightarrow{B_{Earth}}$ is the geocentric magnetic flux density ($Wb \cdot m^{-2}$)

• \vec{m} is the sum of all the satellite's permanent and induced magnetic moments

Apart from attitude control, the magnetic torque is negligible. Besides, we will only focus on passive stabilization of the satellite's attitude. Therefore, we won't consider this torque.

3.4 Equations of motion

The equations of motion for orbit are given by Newton's second law of motion, whose vector expression is given by :

$$m_B \overrightarrow{a_B} = \overrightarrow{F_{drag}} + \overrightarrow{F_{SRP}} + \overrightarrow{F_{grav}}$$

where • $\overrightarrow{F_{grav}}$ is the sum of gravitational forces from all considered attractors

• $\overrightarrow{a_B} = \frac{d\overrightarrow{V_B}}{dt}$ is the acceleration of the system in the ECI frame

Attitude

The equations of motion for attitude are given by Euler's equations, whose expressions are given by :

$$\begin{cases} I_{G_B} \overrightarrow{\omega_B} + \overrightarrow{\omega_B} \wedge (I_{G_B} \overrightarrow{\omega_B}) = \overrightarrow{M_{drag}} + \overrightarrow{M_{SRP}} + \overrightarrow{M_{grav}} \\ \dot{q} = \frac{1}{2} q \triangle \overrightarrow{\omega_B} \end{cases}$$

where • $\overrightarrow{M_{grav}}$ is the sum of moments from all attractors

• $q \triangle \overrightarrow{\omega_B}$ is the Grassmann product of quaternions q and $[0, \overrightarrow{\omega_B}]$

After computing all the terms of this equation, we can eventually integrate them over time thanks to Runge-Kutta 4 method.

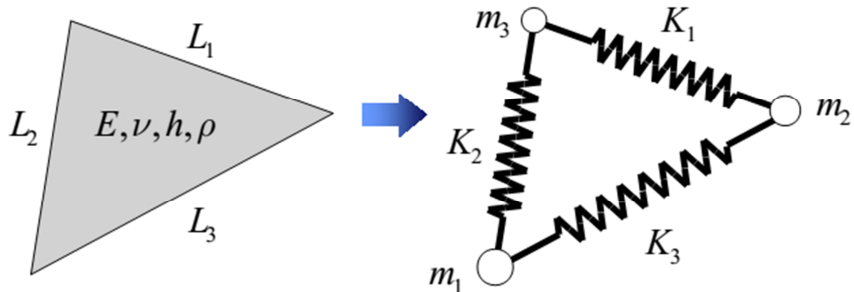
4 Improved Model of the Satellite

In this section, we will give details about an improved version of the above mentioned rigid-body model. We expect the flexibility of both film and tethering convex tapes to dissipate energy, thus reducing potential oscillations. Since the rigid-body model doesn't include that phenomenon, we will try to add the flexibility of the film to it.

4.1 Mass-Spring Network Approximation

Modeling the behavior of the film would normally requires a finite element resolution but it is usually very costly in terms of memory and CPU time. Therefore, we will use a mass-spring network approximation of the finite element analysis that is suggested in a paper from JAXA [17]. We will here detail the proof of the formula given in that paper.

Let's consider a triangular membrane element which we will try to approximate by a mass-spring network.



For each side $i \in [|1,3|]$, let

- K_i : spring constant associated to side i
- L_i : unstressed length of side i

First, we must evenly distribute the mass of the triangular membrane element of unstressed surface S to each corner $\in [|1,3|]$:

$$m_k = m = \frac{\rho S h}{3}$$

The above mentioned approximation consists in determining $K_i, i \in [|1,3|]$ so that, in the case of a uniaxial stress in the direction of any side of the triangular element, the strain energy in the finite element analysis is equal to the spring energy in the approximation.

Let's assume that the triangular membrane element is undergoing a uniaxial deformation $\varepsilon_0 = \frac{\sigma_0}{E}$ in the direction of strain σ_0 , where E is Young's modulus of the membrane.

The expression of the strain energy in the case of a finite element analysis is :

$$\Pi_{strain} = \frac{1}{2} ESh\varepsilon_0^2$$

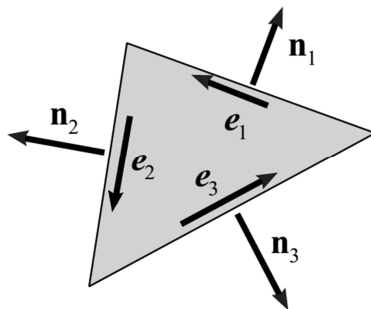
The expression of the energy stored in the springs in the case of the approximation is :

$$\Pi_{springs} = \frac{1}{2} {}^t\varepsilon \begin{pmatrix} K_1 L_1^2 & 0 & 0 \\ 0 & K_2 L_2^2 & 0 \\ 0 & 0 & K_3 L_3^2 \end{pmatrix} \varepsilon$$

where • $\varepsilon = {}^t[\varepsilon_1 \quad \varepsilon_2 \quad \varepsilon_3]$

- for $j \in [|1,3|]$, ε_j is the deformation rate of side j

Let's define unit vectors \vec{e}_i and \vec{n}_i as illustrated in the figure below. Vector \vec{e}_i is defined along the direction of side i and vector \vec{n}_i is normal to side i .



If the stress is parallel to \vec{e}_i , then the expression of the deformation tensor in the $(\vec{n}_i, \vec{e}_i, \vec{e}_z)$ is given by

$$\underline{\underline{\varepsilon}} = \begin{pmatrix} -\nu\varepsilon_0 & 0 & 0 \\ 0 & \varepsilon_0 & 0 \\ 0 & 0 & 0 \end{pmatrix}_{(\vec{n}_i, \vec{e}_i, \vec{e}_z)}$$

where ν is the membrane's Poisson's ratio. Indeed, ε_0 is the deformation along \vec{e}_i and $-\nu\varepsilon_0$ is the deformation along \vec{n}_i .

Then, the deformation rate of side $j \in [|1,3|]$ is given by :

$$\varepsilon_j = {}^t \vec{e}_j \underline{\underline{\varepsilon}} \vec{e}_j$$

which can be re-written as follows :

$$\begin{aligned} \varepsilon_j &= \vec{e}_j \cdot (-\nu\varepsilon_0(\vec{e}_j \cdot \vec{n}_i)\vec{n}_i + \varepsilon_0(\vec{e}_j \cdot \vec{e}_i)\vec{e}_i) \\ &= \varepsilon_0(\vec{e}_i \cdot \vec{e}_j)^2 - \nu\varepsilon_0(\vec{n}_i \cdot \vec{e}_j)^2 \\ &= \varepsilon_0 \cos^2((\vec{e}_i, \vec{e}_j)) - \nu\varepsilon_0 \cos^2((\vec{n}_i, \vec{e}_j)) \\ &= \varepsilon_0 \cos^2((\vec{e}_i, \vec{e}_j)) - \nu\varepsilon_0 \cos^2((\vec{e}_i, \vec{e}_j) + \frac{\pi}{2}) \\ &= \varepsilon_0 \cos^2((\vec{e}_i, \vec{e}_j)) - \nu\varepsilon_0 \sin^2((\vec{e}_i, \vec{e}_j)) \\ &= \varepsilon_0(1 - \sin^2((\vec{e}_i, \vec{e}_j))) - \nu\varepsilon_0 \sin^2((\vec{e}_i, \vec{e}_j)) \\ &= \varepsilon_0(1 - (1 + \nu) \sin^2((\vec{e}_i, \vec{e}_j))) \end{aligned}$$

Given the expression of the triangle's surface (true if $i \neq j$),

$$S = \frac{1}{2} L_i L_j \sin((\vec{e}_i, \vec{e}_j))$$

We can give an expression of angle (\vec{e}_i, \vec{e}_j)

$$\sin^2((\vec{e}_i, \vec{e}_j)) = \begin{cases} \frac{4S^2}{L_i^2 L_j^2} & \text{if } i \neq j \\ 0 & \text{if } i = j \end{cases}$$

Which yields

$$\varepsilon_j = \varepsilon_0 p_{ij}$$

where

- $p_{ij} = 1 - \frac{4(1+\nu)S^2}{L_i^2 L_j^2} \delta_{ij}$
- $\delta_{ij} = \begin{cases} 1 & \text{if } i \neq j \\ 0 & \text{if } i = j \end{cases}$

Next, we can re-write the condition on energies for each of the three sides $\in [|1,3|]$:

$$\begin{aligned}\Pi_{springs} = \Pi_{strain} &\iff \forall i \in [|1,3|], \quad \frac{1}{2} ESh \varepsilon_0^2 = \frac{1}{2} \sum_{j=1}^3 \varepsilon_0^2 p_{ij}^2 L_j^2 K_j \\ &\iff \forall i \in [|1,3|], \quad ESh = \sum_{j=1}^3 p_{ij}^2 L_j^2 K_j\end{aligned}$$

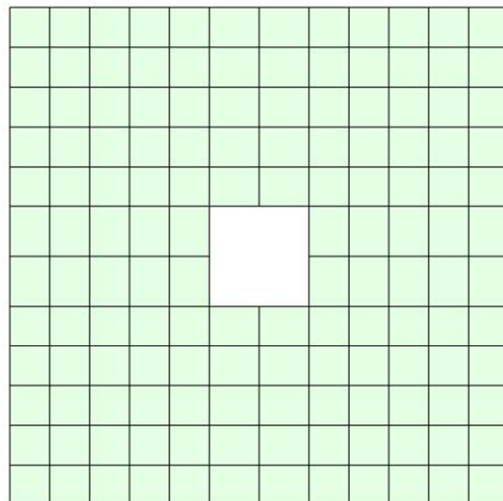
Which finally yields the expression of the spring constants :

$$\begin{pmatrix} K_1 \\ K_2 \\ K_3 \end{pmatrix} = B^{-1} \begin{pmatrix} 1 \\ 1 \\ 1 \end{pmatrix}$$

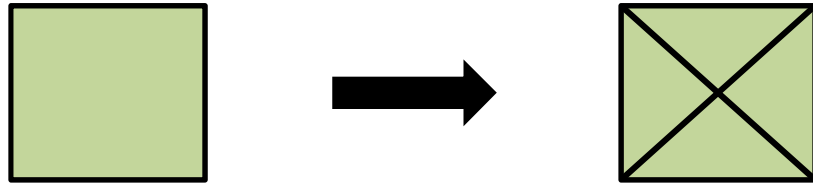
where • $B = (B_{ij})_{(i,j) \in [|1,3|]^2}$
• $B_{ij} = \frac{p_{ij}^2 L_j^2}{ESh}$

4.2 Internal Forces

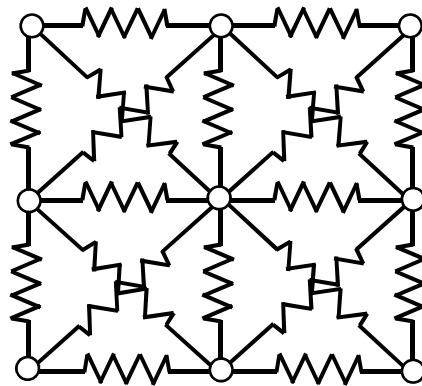
The method to model the film and compute the internal forces works as follows. We must first create a rectangular mesh that takes into account the boundaries of the film, as the one illustrated below.



Then each rectangular element will be divided in four triangles as illustrated below.



After that, each triangle will be modeled individually by the mass-spring approximation explained in section 4.1, and we will superpose spring constants on adjacent edges and superpose particles masses on vertices, to obtain a mass-spring network of the same type as the one illustrated below.



Therefore, each node i will be undergoing from a spring force from its neighbors :

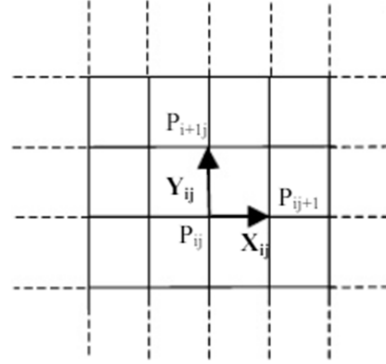
$$\overrightarrow{F_{int}} = \sum_{j \in A_i} -k_{ij} (\|\vec{r}_i - \vec{r}_j\|_2 - L_{ij}) \overrightarrow{u_j}$$

where

- k_{ij} is the spring constant linking nodes i and j
- L_{ij} is the unstressed length of the spring linking nodes i and j
- \vec{r}_i and \vec{r}_j are the position vectors of respectively nodes i and j in ECI frame
- A_i is the set of nodes that are neighbors of node i
- $\overrightarrow{u_j} = \frac{\vec{r}_i - \vec{r}_j}{\|\vec{r}_i - \vec{r}_j\|_2}$

4.3 Modified Computation of SRP and Drag Forces

Now that we have a meshed flexible film, we can proceed to a more accurate computation of SRP and drag forces. Thus, we need to define a surface an orthonormal vector for each mas particle of the film. To do so, we will use the method mentioned in a PhD thesis dedicated to modeling the motion of fabric [3].



To calculate the area A_{ij} associated to particle P_{ij} , we will proceed as follows :

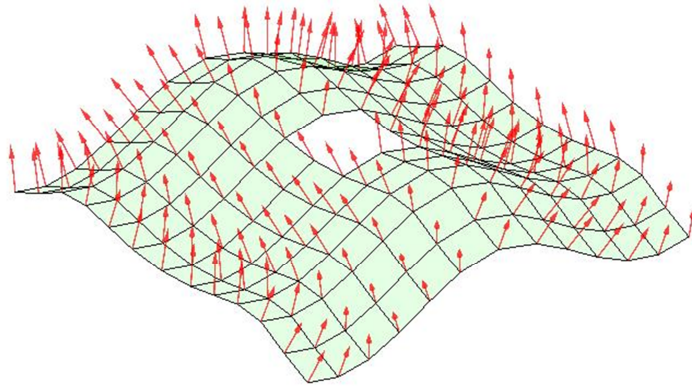
$$A_{ij} = \frac{1}{\text{card}(E_{ij})} \sum_{(k,l) \in E_{ij}} \left\| \overrightarrow{X_{kl}} \wedge \overrightarrow{Y_{kl}} \right\|$$

where • E_{ij} is the set of faces whose vertices include P_{ij}
 • $\text{card}(E_{ij})$ is the number of faces in set E_{ij}

To calculate the normal unit vector $\overrightarrow{n_{ij}}$ associated to A_{ij} , and thus to E_{ij} , we will proceed as follows :

$$\overrightarrow{n_{ij}} = \frac{1}{\left\| \sum_{(k,l) \in E_{ij}} \overrightarrow{X_{kl}} \wedge \overrightarrow{Y_{kl}} \right\|} \sum_{(k,l) \in E_{ij}} \overrightarrow{X_{kl}} \wedge \overrightarrow{Y_{kl}}$$

After doing so, we obtain film modeled as a mass-spring network with a set of sub-faces and their associated normal unit vector (for both front and back sides of the film), as illustrated below.



From there we can calculate, for each particle (i, j) , SRP and drag force using the formulae explained in sections 3.3.2 and 3.3.3, and add them to compute the orbit and attitude of the whole system.

4.4 Equations of Film Behavior

As for the equations for the behavior of the film, they basically consist in writing Newton's second law of motion on every node :

$$m_k \vec{a}_k = \vec{F}_{int}^k + \vec{F}_{drag}^k + \vec{F}_{grav}^k + \vec{F}_{SRP}^k$$

where • m_k is the mass of node k

• a_k is the acceleration of node k in ECI frame

To solve them numerically, we will also integrate them over time with Runge-Kutta 4. However, we shouldn't forget to numerically "fix" the four corners of the film to the rigid structure to run computations.

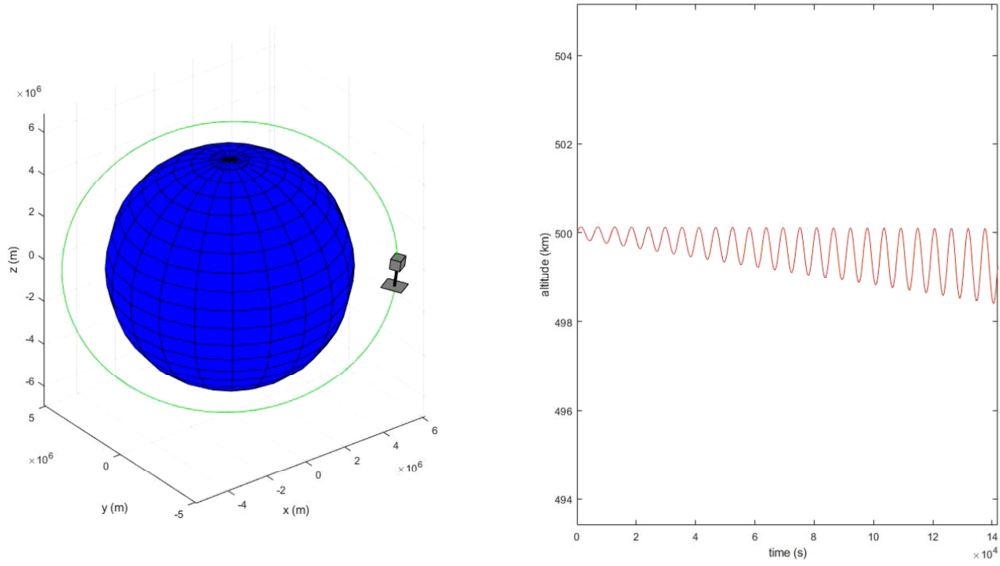
5 Results and Discussions

In that section, we will provide some results from the above mentioned models as well as some discussions about their reliability and potential further improvements.

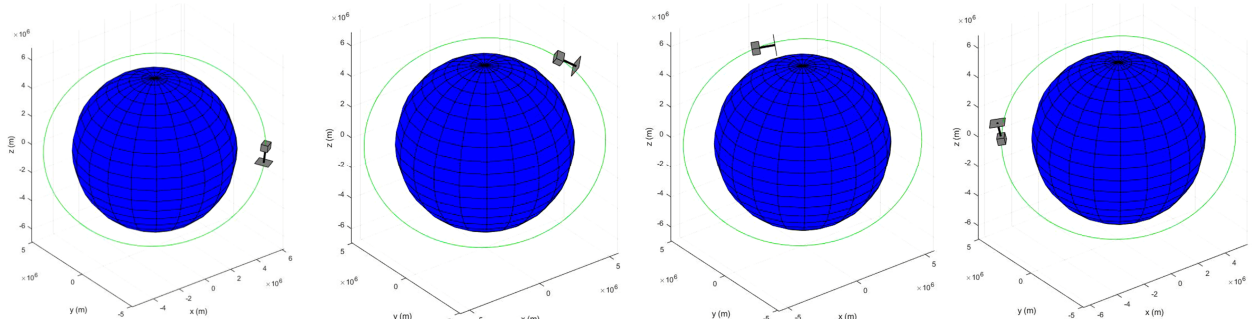
5.1 Results

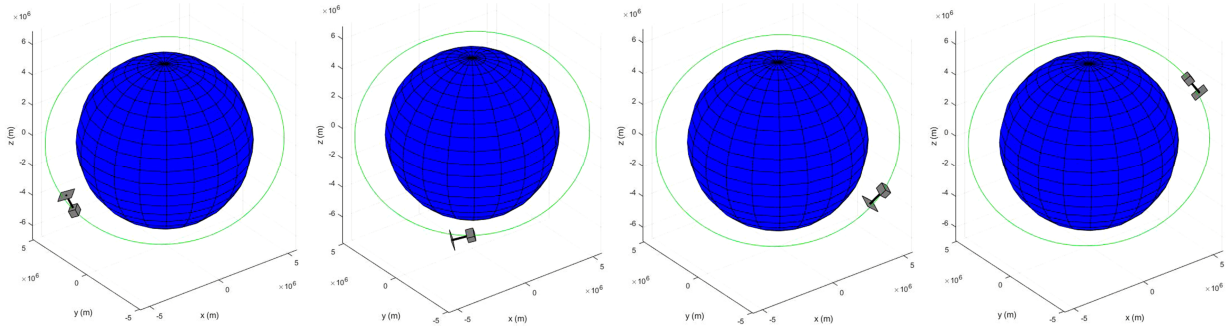
Rigid-body model

Here is the kind of result that we get from the rigid-body model.

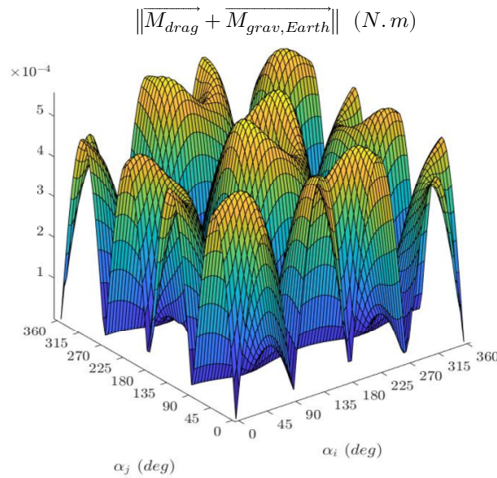


We can see that altitude shows up-and-down oscillations but that it decreases overall. As for attitude, it seems to be stable over time, as suggested by the drag and gravity torque graphs from section 3.3, as illustrated below.



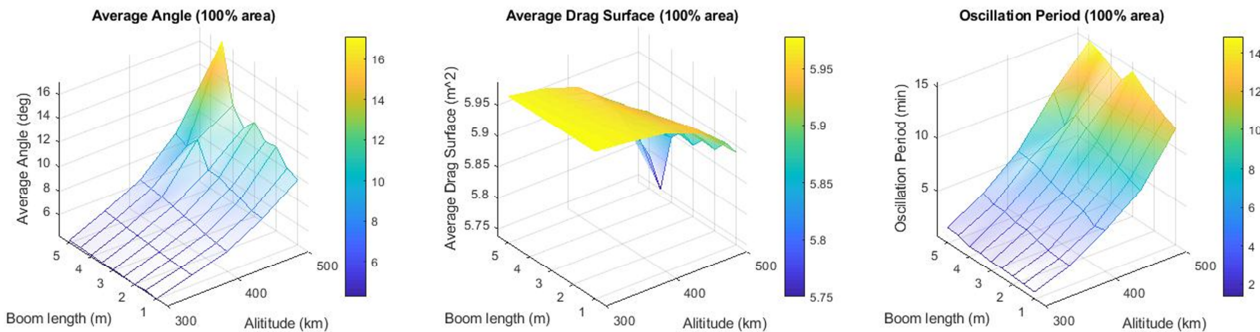


Indeed, when we add drag and gravity torques, we obtain and shift in values but overall, the graph still shows "zeros" values, which is why the above represented attitude seems stable, with a film that remains behind the satellite.



Boom Length

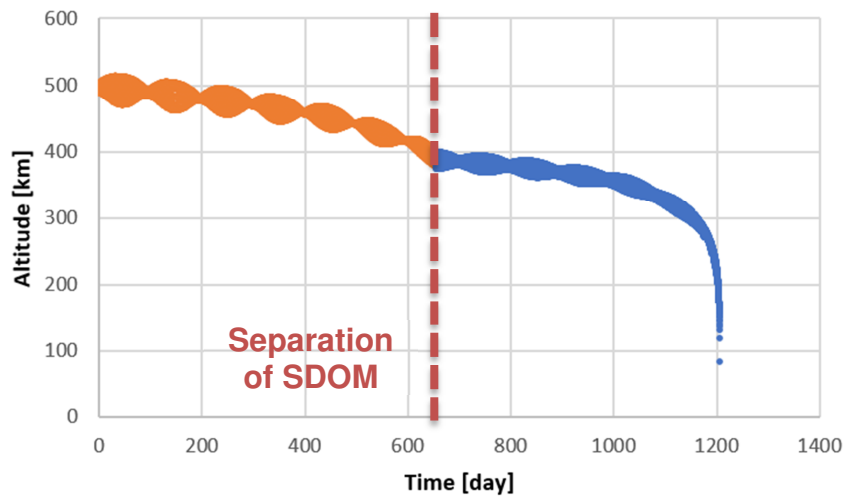
To decide on the length of convex tapes, we aimed at minimizing the necessary time span to complete the orbit decay. To do so, we need to maximize the drag force, and thus maximize the average effective drag area. For that we proceeded to a parameter analysis of the oscillation period (determined by Fourier transform), the average angle (\vec{k}, \vec{V}_B) and the average effective drag surface depending on altitude and boom length.



We can see that both average angle and average drag surface significantly increases when altitude and boom length increase. Thus, we must take that into account to decide on boom length, along with shading of solar panels depending on boom length.

Time span for orbit decay

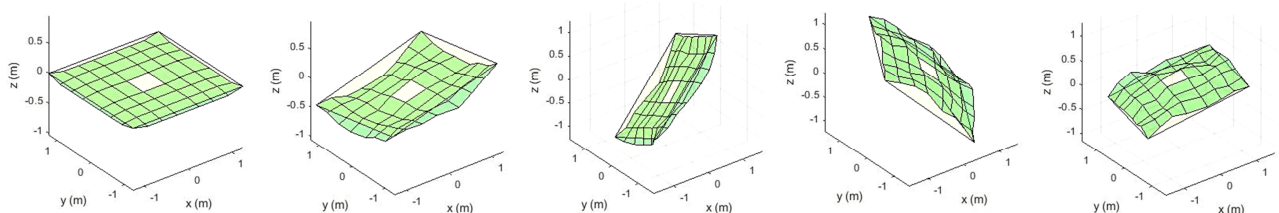
To estimate the time span for orbit decay, in our case from 500 km down to 400 km of altitude, we ran a simulation over several days. We also computed the orbit after separation of the SDOM. The results are shown in the chart below.



As illustrated above, preliminary results show that the orbit decay performed with SDOM might take about two years. Nonetheless, further simulations should be run with more accurate models to confirm the relevance of this result.

Film behavior

The mass-spring network approximation provided nice results for both surface force computation and the motion of the film itself. Here are some pictures of the computed behavior of the film over the first few minutes of the simulated orbit.



5.2 Potential Improvements

Behavior of the film

Preliminary simulations showed that the mass-spring network approximation has poor stability properties. Indeed, the integration time step is not small enough, or when the film's Young's modulus is too high, the computed solution diverges. Thus, we might consider implementing sub time steps to compute the behavior of the film, while considering that all other variables are constant between two "big" time steps.

Behavior of the convex tapes

So far, we have considered that the convex tapes tethering the satellite to the film were rigid, which is not exactly true. Indeed, convex tapes have a behavior that is hard to predict. Notably, it is pretty weak to torsion. However, PhD theses from French Ecole Centrale de Marseille [7] [10] provide a method to model and compute the behavior of convex tapes used for space-related purposes.

These papers provide expressions for the tapes' energies, from which we should, in our case, deduce the equations of motion using Hamilton's principle. Even though such expressions are quite heavy, which makes using Hamilton's principle quite difficult and very costly in terms of CPU time because it would eventually require solving partial differential equations, it is necessary to take that behavior into account.

6 Conclusion

To compute the orbit and attitude of ALEe satellite during its orbit decay performed with a deployed SDOM, two numerical models have been implemented. It involved a numerical method to compute the necessary forces has been included and refined in the case of the flexible drag sail. Note that the physical model for the drag sail has been inspired from methods use in fabric modeling and solar sail modeling.

These models have provided preliminary results and enabled an estimation of the necessary time span to complete the orbit decay.

To refine this model, further improvements could be added, such as "sub" time steps to compute the motion of the film and implementation of the motion of the convex tapes.

References

- [1] Re-Entry: FREEDOM Drag Sail CubeSat – Spaceflight101, (n.d.).
<https://spaceflight101.com/re-entry/freedom/> (accessed June 18, 2018).
- [2] Y. Miyazaki, Dynamics Model of Solar Sail Membrane, Nihon University, Chiba 274-8501, Japan, 2004. http://www.hayabusa.isas.jaxa.jp/kawalab/astro/pdf/2004A_6.pdf (accessed June 18, 2018).
- [3] T. El Hassane, CARACTERISATION, MODELISATION ET SIMULATION DU COMPORTEMENT D'UN TISSU TEXTILE, UNIVERSITE BORDEAUX I, 2001.
<https://fr.scribd.com/doc/15771813/CARACTERISATION-MODELISATION-ET-SIMULATION-DU-COMPORTEMENT-D-UN-TISSU-TEXTILE> (accessed June 18, 2018).
- [4] M. Vajiha, P. Pedram, Mass spring parameters identification for knitted fabric simulation based on FAST testing and particle swarm optimization, (2016).
<https://link.springer.com/content/pdf/10.1007%2Fs12221-016-6567-8.pdf> (accessed June 18, 2018).
- [5] Z. Paweł, Modeling disturbances influencing an Earth-orbiting satellite, (2012).
http://www.par.pl/2012/PAR_05_2012_Zagorski_98_103.pdf (accessed June 18, 2018).
- [6] L. Pirovano, P. Seefeldt, B. Dachwald, R. Noomen, ATTITUDE AND ORBITAL DYNAMICS MODELING FOR AN UNCONTROLLED SOLAR-SAIL EXPERIMENT IN LOW-EARTH ORBIT, in: München, Germany, 2015.
http://issfd.org/2015/files/downloads/papers/079_Pirovano.pdf (accessed June 18, 2018).
- [7] P. Marone-Hitz, Modeling of spatial structures deployed by tape springs : Towards a home-made modeling tool based on rod models with flexible cross sections and asymptotic numerical methods, Ecole Centrale de Marseille, 2014. https://tel.archives-ouvertes.fr/tel-01152819/file/Diffusion_Hitz.pdf (accessed June 18, 2018).
- [8] Euler's equations (rigid body dynamics), Wikipedia. (2018).
[https://en.wikipedia.org/w/index.php?title=Euler%27s_equations_\(rigid_body_dynamics\)&oldid=821254510](https://en.wikipedia.org/w/index.php?title=Euler%27s_equations_(rigid_body_dynamics)&oldid=821254510) (accessed June 18, 2018).
- [9] Angles d'Euler, Wikipédia. (2018).
https://fr.wikipedia.org/w/index.php?title=Angles_d%27Euler&oldid=145915052 (accessed June 18, 2018).
- [10] P. Marone-Hitz, B. Cochelin, S. Bourgeois, F. Guinot, Modélisation de structures multi-rubans pour applications spatiales, in: 11e Colloque National En Calcul Des Structures, Presqu'île de Giens, France, 2013. <https://hal.archives-ouvertes.fr/hal-01320045> (accessed June 18, 2018).
- [11] E. PICHAULT, A rod model with flexible thin-walled cross-section. Application to the folding of tape springs in 3D, PhD Thesis, UNIVERSITE D'AIX-MARSEILLE, 2013.
<https://tel.archives-ouvertes.fr/tel-00921931/document> (accessed June 18, 2018).

- [12] Conversion between quaternions and Euler angles, Wikipedia. (2018).
https://en.wikipedia.org/w/index.php?title=Conversion_between_quaternions_and_Euler_angles&oldid=828712576 (accessed June 18, 2018).
- [13] E. A. Coutsias, L. Romero, The Quaternions with an application to Rigid Body Dynamics, (1999). <http://www.ams.stonybrook.edu/~coutsias/papers/rrr.pdf> (accessed June 18, 2018).
- [14] M. Indrek, Rigid body dynamics using Euler's equations, Runge-Kutta and quaternions, (2008). <http://www.mare.ee/indrek/varphi/vardyn.pdf> (accessed June 18, 2018).
- [15] N. Dantam, dantam-quaternion.pdf, (2014). <http://www.neil.dantam.name/note/dantam-quaternion.pdf> (accessed June 18, 2018).
- [16] K. Lu, M. Accorsi, J. Leonard, Finite element analysis of membrane wrinkling, International Journal for Numerical Methods in Engineering. 50 (n.d.) 1017–1038. doi:10.1002/1097-0207(20010220)50:5<1017::AID-NME47>3.0.CO;2-2.
- [17] S. Bilbao, O. Thomas, C. Touzé, M. Ducceschi, Conservative Numerical Methods for the Full von Kármán Plate Equations, Numerical Methods for Partial Differential Equations. (2015) 1–23. doi:10.1002/num.21974.
- [18] N. Damil, M. Potier-Ferry, H. Hu, New nonlinear multiscale models for wrinkled membranes, (2013). <https://hal.archives-ouvertes.fr/hal-00823921> (accessed June 18, 2018).
- [19] ALE Co., Ltd, press_ale, (2017).
https://www.dropbox.com/sh/tsbr07mv7vy1nld/AAAzaq9kiZW91_ZX9WzrLOIa?dl=0&prevew=ALE+Co.%2C+Ltd.+Company+Overview.pdf (accessed June 19, 2018).
- [20] SHOOTING STAR challenge, SHOOTING STAR challenge. (2017).
<http://shootingstarchallenge.com> (accessed June 19, 2018).
- [21] ALE Co., Ltd, ALE Co., Ltd. — Shooting stars. On demand. The Future of Entertainment in Space., (n.d.). <http://star-ale.com/en/> (accessed June 19, 2018).
- [22] Earth-centered inertial - Wikipedia, (n.d.). https://en.wikipedia.org/wiki/Earth-centered_inertial (accessed June 22, 2018).